The Q_{weak} Experiment: First Direct Measurement of the Weak Charge of the Proton

2016 J. Phys.: Conf. Ser. 678 012026

(http://iopscience.iop.org/1742-6596/678/1/012026)

The Q_{weak} Experiment: First Direct Measurement of the Weak Charge of the Proton

J.F. Dowd for the Q_{weak} Collaboration
College of William and Mary, Williamsburg, VA 23185 USA
E-mail: jdowd@jlab.org

Abstract. The recently completed Q_{weak} experiment at Jefferson Laboratory made the first direct determination of the proton's weak charge, Q_W^p, via a measurement of the parity-violating asymmetry in elastic electron-proton scattering at low four-momentum transfer. The Standard Model (SM) makes a precise prediction of $Q_W^p(SM) = 0.0710 \pm 0.0007$. A deviation from this prediction could be an indicator of new physics. A longitudinally polarized electron beam was scattered off a liquid hydrogen target and detected in eight azimuthally symmetric fused silica detectors. The small asymmetry, $A_{ep} = -279 \pm 35$ (stat) ± 31 (syst) ppb, was measured by observing the difference in rates seen in the detectors when the helicity of the electron beam was rapidly reversed. The measured asymmetry is the most precise and smallest asymmetry ever measured in an $\vec{e}p$ scattering experiment. Combining this asymmetry with previous parity-violating electron scattering (PVES) data, we obtained a value of $Q_W^p(PVES) = 0.064 \pm 0.012$, which agrees well with the SM value. The results of the experiment's commissioning run, which constitutes about 4% of the total data set, are reported here. Analysis of the remainder of the data set is ongoing and will significantly reduce the statistical and systematic uncertainties; several aspects of this analysis will be highlighted.

1. Introduction

The Standard Model (SM) is an undeniably effective theoretical framework of particle physics. Due to the existence of dark matter and the inability to explain the large observed matter/anti-matter asymmetry in the universe, the SM is thought to be an effective low-energy theory of more fundamental higher-energy physics. Exploration of possible physics beyond the SM include direct searches at the energy frontier and indirect searches at the precision frontier. The weak charge of the proton is suppressed and well-predicted in the SM, which increases its sensitivity to possible new physics and makes it an excellent candidate for a precision measurement [1].

The weak charge of the proton emerges from the SM Lagrangian through the axial electron, vector quark weak couplings, $C_{1i} = 2g_A^e g_V^i$. At tree-level, Q_w^p is given by

$$Q_w^p = -2(2C_{1u} + C_{1d}) = 1 - 4\sin^2\theta_W \tag{1}$$

where θ_W is the Weinberg angle, or electroweak mixing angle. The proton's weak charge is the neutral-weak analog to the proton's electric charge.

The observable quantity measured in this experiment is the parity-violating (PV) asymmetry, A_{ep}, formed from the difference over the sum of elastic $\vec{e}p$ scattering cross sections with positive and negative helicity, given by

$$A_{ep} = \frac{\sigma_+ - \sigma_-}{\sigma_+ + \sigma_-}. \tag{2}$$

At tree-level and in terms of electromagnetic, and vector and axial-vector neutral-weak form factors, the PV asymmetry is

$$A_{ep} = \left[\frac{-G_F Q^2}{4\pi\alpha\sqrt{2}}\right]\left[\frac{\varepsilon G_E^\gamma G_E^Z + \tau G_M^\gamma G_M^Z - (1-4\sin^2\theta_W)\varepsilon' G_M^\gamma G_A^Z}{\varepsilon (G_E^\gamma)^2 + \tau (G_M^\gamma)^2}\right] \tag{3}$$

where

$$\varepsilon = \frac{1}{1+2(1+\tau)\tan^2\frac{\theta}{2}}, \qquad \varepsilon' = \sqrt{\tau(1+\tau)(1-\varepsilon^2)} \tag{4}$$

are kinematic quantities. G_F is the Fermi constant, θ_W is the weak mixing angle, θ is the laboratory electron scattering angle, $-Q^2$ is the four-momentum transfered squared, M is the proton mass, and $\tau = Q^2/4M^2$. At low Q^2 and in the forward angle limit, $\theta \to 0$, the asymmetry simplifies and can be recast into the reduced asymmetry

$$A_{ep}/A_0 = Q_w^p + Q^2 B(Q^2,\theta), \qquad A_0 = \left[\frac{-G_F Q^2}{4\pi\alpha\sqrt{2}}\right]. \tag{5}$$

The second term in the reduced asymmetry, $Q^2 B(Q^2,\theta)$, contains all of the hadronic structure and is suppressed at low Q^2. It was determined from previous PVES experiments at higher Q^2. The first term, Q_w^p, is then the intercept when the asymmetry is plotted versus Q^2.

Looking beyond tree level, with electroweak radiative corrections applied, the SM prediction of Q_w^p at $Q^2 = 0$ is

$$Q_w^p(SM) = [\rho_N C + \Delta_e][1 - 4\sin^2\hat{\theta}_W(0) + \Delta_e'] + \Box_{WW} + \Box_{ZZ} + \Box_{\gamma Z}(0). \tag{6}$$

Here, ρ_{NC} renormalizes the ratio of neutral to charged-current interactions at low energies [1]. Δ_e and Δ_e' are corrections to the Zee and γee couplings at the electron vertex. $\Box_{WW}$ and $\Box_{ZZ}$ are exchanges of two of the same weak boson that are easily calculable with perturbative quantum chromodynamics (QCD). The final correction, $\Box_{\gamma Z}$, is the dominant energy-dependent correction to equation 5 at the experiment's kinematics. This energy-dependent contribution must be subtracted from the Q_{weak} measurement to be compared with the SM prediction. Refinement of the $\Box_{\gamma Z}$ calculation is ongoing and has been evaluated by several groups (see Table 1). The most recent calculation [7], used to correct the data introduced here, uses parton distribution functions in combination with recent $\vec{e}d$ scattering data [9] to make the most precise calculation of $\Box_{\gamma Z}$ to date.

Presented here is the analysis of the commissioning run (approximately 4% of our total dataset) of the Q_{weak} experiment, which measured the parity-violating asymmetry in $\vec{e}p$ scattering to high precision. Combined with results from previous parity-violating electron scattering experiments (PVES), these data were used as a direct measurement of Q_w^p. The combination of C_{1u} and C_{1d} contained in Q_w^p is nearly orthogonal to that found in atomic parity violation (APV) experiments on ^{133}Cs [2], where $Q_w(^{133}\mathrm{Cs}) = -2(188\mathrm{C_{1u}} + 211\mathrm{C_{1d}})$.

Table 1. $\Box_{\gamma Z}^V(E,Q^2)$ contribution to Q_w^p at Q_{weak} kinematics

Gorchtein & Horowitz [3]	0.0026 ± 0.0026
Sibirtsev, Blunden, Melnitchouk, & Thomas [4]	$0.0047^{+0.0011}_{-0.0004}$
Rislow & Carlson [5]	0.0057 ± 0.0009
Gorchtein, Horowitz, & Ramsey-Musolf [6]	0.0054 ± 0.0020
Hall, Blunden, Melnichouk, Thomas, & Young [7]	0.00557 ± 0.00036

The complementarity of these two measurements provides a clean extraction of the individual light quark weak charges and, therefore, also allows a determination of the weak charge of the neutron, $Q_w^n = -2(C_{1u} + 2C_{1d})$.

2. Experimental Overview

The custom Q_{weak} apparatus [10] (Figure 1) was installed in Hall C of Jefferson Lab, a continuous electron beam accelerator facility [11]. The main components were a 34.4 cm long LH_2 target, a triple collimator system, toroidal magnetic spectrometer, and eight fused silica Cerenkov detectors arrayed around the beam axis. Retractable wire drift chambers, before and after the magnet, were used at low beam current to track individual scattered electrons and characterize the Q^2 of the experiment.

At the target center, the 89 ± 1.8% longitudinally polarized 145 μA electron beam had an average energy of 1.155 ± 0.003 GeV. The helicity of the electrons was rapidly reversed at 960 Hz in a pseudo-random quartet pattern, either (+ - - +) or (- + + -). The rapid reversal limited noise due to target density fluctuations, and the quartet reversal pattern reduced noise due to slow linear drifts. Precision beam polarimetry for the commissioning period was provided by an existing Møller polarimeter. This measurement was invasive and was limited to low beam currents (about 1 μA). For the final result, the Møller polarimeter measurement will be crosschecked with a new Compton polarimeter built specifically for the Q_{weak} experiment. The Compton polarimetery measurement is non-invasive and can be performed continuously at beam currents up to 180 μA.

The 34.4 cm long, conical, aluminum target cell was designed using computational fluid dynamics to minimize density fluctuations from the deposition of heat from the high energy and high current beam. The electron beam was incident on the high-power (3 kW) LH_2 target and was uniformly rastered over an area of 3.5 x 3.5 mm^2 to improve heat dissipation at the thin aluminum target windows, yielding a very high luminosity, of order 10^{39} cm^{-2}s^{-1}. The target density fluctuations contributed about 40 ppm to the measured asymmetry width per quartet.

The acceptance of the experiment was defined by the triple-collimator system, with an effective elastic scattering angle of 7.9 ± 3°. Upon scattering from the target, forward angle electrons pass through the collimators, where the toroidal magnet focuses elastically scattered electrons onto the detectors, while simultaneously diverting inelastics to larger radii. In the azimuthal direction, the experiment's acceptance is about 50% of 2π.

Eight radiation-hard quartz Cerenkov detectors were arrayed symmetrically about the beam axis. Each detector was comprised of two 100 x 16 x 1.25 cm bars glued together to make a 2 m long bar, two photo-multiplier tubes (PMTs), and a pre-radiator. The 2 cm thick lead

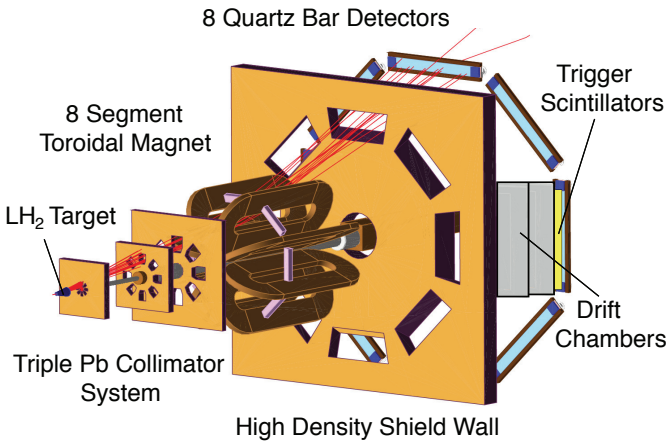

Figure 1. Schematic view of the Q_{weak} experiment showing the target, collimators, toroidal magnet, and detectors. Elastically scattered electrons (red lines) are focused at the detectors, while inelastically scattered electrons (not shown) are bent away to higher radii.

pre-radiators were installed to suppress soft backgrounds and amplify the electron signal. The average light yield of an elastically scattered electron event was about 90 photo-electrons. The octagonal symmetry arrangement was chosen to suppress helicity-correlated beam motion effects when extracting the asymmetry.

In addition, there exists a smaller Q_{weak} data set with a beam current of 3.35 GeV, a Q^2 of 0.09 $(\mathrm{GeV})^2$, and a missing mass $W \approx 2.2$ GeV. The chosen kinematics allows access to non-resonant inelastic $\vec{e}p$ scattering, where the asymmetry depends on the $F_{1,3}^{\gamma Z}$ structure functions used in $\Box_{\gamma Z}$ calculations. The large missing mass leads to a significant background of pions that enter the acceptance of the experiment and hit the Cerenkov detectors. A 10 cm thick lead wall was placed in front of one Cerenkov detector to attenuate the scattered electrons and isolate the pions. Combining this with a pulse height analysis of all eight detectors, the pion background will be separated from the inelastic signal of interest. The polarized beam had a large transverse component which dilutes the parity-violating inelastic asymmetry. This contribution has been measured and characterized with dedicated transversely polarized beam (≈100%). Analysis of this data will provide experimental validation of the theoretical models used to predict the $\Box_{\gamma Z}$ contribution to the weak charge of the proton and will be presented in an upcoming thesis.

3. Analysis

The charge normalized detector light yield was integrated over each stable helicity state, $Y_{\pm}$, in each quartet to form a raw asymmetry,

$$A_{raw} = \frac{Y_+ - Y_-}{Y_+ + Y_-}. \tag{7}$$

The raw asymmetry was corrected for sources of false asymmetries to extract the measured asymmetry,

$$\begin{aligned} A_{msr} &= A_{raw} + A_T + A_L - \sum_{i=1}^{5} \left(\frac{\partial A}{\partial \chi_i} \right) \Delta\chi_i \\ &= A_{raw} + A_T + A_L + A_{reg}. \end{aligned} \tag{8}$$

A_T is due to the small residual transverse polarization in the nominally longitudinally polarized beam. A_T is highly suppressed by the azimuthal symmetry of the detector system and is explicitly measured with dedicated transversely polarized beam. A_L accounts for possible non-linearities in the PMT response. In the final term, the $\Delta\chi_i$ are helicity-correlated differences in beam trajectory or energy in a quartet. The slopes $\frac{\partial A}{\partial \chi_i}$ were determined using linear regression of natural beam motion. For the data presented here, $A_T = 0 \pm 4$ ppb, $A_L = 0 \pm 3$ ppb, and $A_{reg} = -35 \pm 11$ ppb. After these corrections are applied the resulting measured asymmetry is $A_{meas} = -204 \pm 31$ ppb (stat) ± 13 ppb (syst).

The PV elastic $\vec{e}p$ asymmetry, A_{ep}, was then extracted from A_{meas} by,

$$A_{ep} = R_{Tot} \frac{A_{meas}/P - \sum_{i=0}^{4} f_i A_i}{1 - \sum f_i}. \tag{9}$$

The overall factor R_{Tot} accounts for the combined effects of radiative corrections, the non-uniformities in light and Q^2 distribution across the detectors, and kinematics normalization. P is the longitudinal polarization of the beam. A_i and f_i are the asymmetries and corresponding dilution factors (fraction of total signal due to background i) for each background. The measured asymmetry was diluted by backgrounds that arose from electrons that scattered off the aluminum target cell windows, the beamline, soft neutral background, and inelastically scattered electrons.

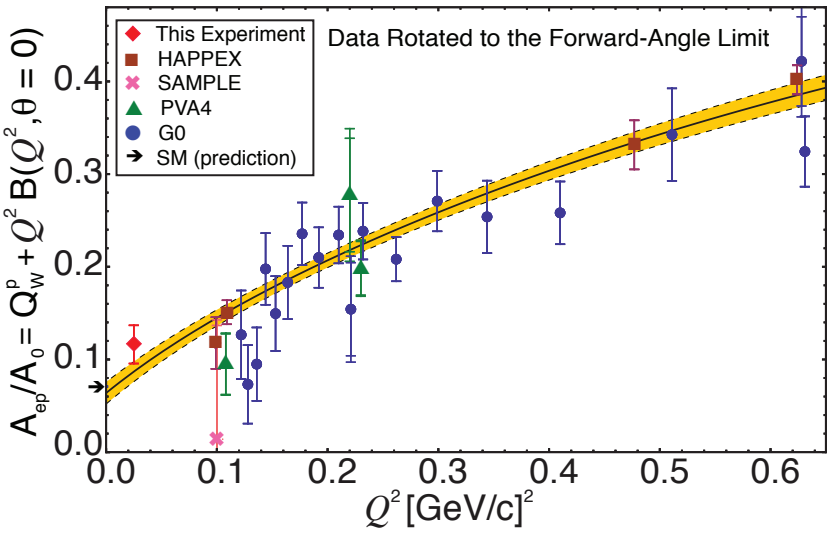

Figure 2. Global fit (black line) of world PVES data including the Q_{weak} commissioning data (red diamond). The outer band (dashed line) represents the uncertainty of the fit. This fit incorporated all PVES measurements including proton, helium, and deuterium data up to $Q^2 = 0.63(\text{GeV})^2$. All data were rotated to the forward angle limit, with the outer error bars indicating the additional uncertainty from the rotation. Q_w^p is the intercept of the fit and the SM prediction is indicated by the black arrow.

Because the detector signals are integrated, we cannot exclude background signals from the signal of interest. Therefore, each background was accounted for, with explicit measurements of their asymmetries and dilution factors and subtracted from the measured asymmetry. By far, the largest background to the measured asymmetry was from the aluminum target cell windows, due to the neutron content of the aluminum, where the measured asymmetry was 1.76 ppm and the dilution factor was 3.2%.

4. Results

Reported here are the results of the Q_{weak} experiment's commissioning run, which represents 4% of the total dataset. The fully corrected asymmetry was $A_{ep} = -279 \pm 35$ (stat) ± 31 (syst) ppb. Following the procedure in references [12] and [13], the asymmetry reported here was combined with existing world PVES data on hydrogen, deuterium, and ^{4}He targets [14–25] in a global fit (Figure 2) of the reduced asymmetry in equation 5. All PVES data up to $Q^2 = 0.63(\text{GeV})^2$ were used. The free parameters of the fit include the light quark weak charges C_{1u} and C_{1d}, the strange charge radius ρ_s, the strange magnetic moment μ_s, and the isovector axial form factor $G_A^{Z(T=1)}$. The value of the isoscalar axial form factor $G_A^{Z(T=0)}$ was constrained by theoretical calculations [26]. The Kelly parametrization [27] was used for the electromagnetic form factors. In addition, all data were corrected for the energy dependence that arises from $\Box_{\gamma Z}$ contributions. The intercept of the fit ($Q^2 = 0$) is $Q_w^p(PVES) = 0.064 \pm 0.012$ in excellent agreement with the SM prediction, $Q_w^p(SM) = 0.0710 \pm 0.0007$. This represents the first direct measurement of the weak charge of the proton.

This measurement of the weak charge of the proton was then used to constrain the weak isoscalar and isovector couplings (see figure 3). Combined with the APV experiments mentioned in section 1, the light quark weak charges were determined to be $C_{1u} = -0.1835 \pm 0.0054$ and $C_{1d} = +0.3355 \pm 0.0050$. These results are in good agreement with the SM predictions, $C_{1u}(SM) = -0.188$ and $C_{1d}(SM) = +0.341$ [28]. The light quark weak charges are in turn used

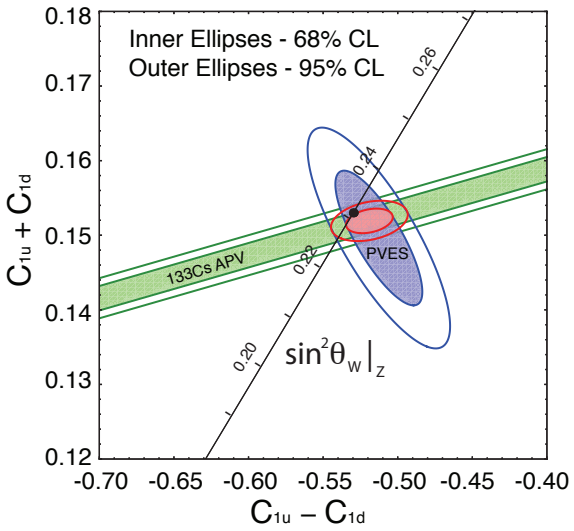

Figure 3. The constraints on the isoscalar $(C_{1u} + C_{1d})$ and isovector $(C_{1u} - C_{1d})$ weak currents from PVES and APV experiments are shown here. The almost horizontal (green) APV band is nearly orthogonal to PVES (blue) ellipse, which allows for a relatively clean extraction of C_{1u} and C_{1d}. The red ellipse shows the result of combining the PVES and APV data. The SM prediction [28] as a function of $\sin^2\theta_W$ in the $\overline{MS}$ scheme is plotted (diagonal black line) with the SM best fit value indicated by the (black) point.

to extract the neutron's weak charge, $Q_w^n(PVES + APV) = 2(C_{1u} + 2C_{1d}) = -0.975 \pm 0.010$, which is also in good agreement with the SM prediction, $Q_w^p(SM) = -0.9890 \pm 0.0007$. This represents the first determination of the weak charge of the neutron.

The commissioning data reported here represents 4% of the total data acquired during the running of the Q_{weak} experiment. The final result when published will benefit from an asymmetry anticipated to have significantly reduced systematic uncertainties and a five times smaller statistical uncertainty.This high-precision asymmetry measurement will provide a test of both the standard model and parity-violating new physics beyond the standard model at the TeV scale [1, 12].

References

[1] J. Erler, A. Kurylov and M. J. Ramsey-Musolf, Phys. Rev. D **68**, 016006 (2003) [hep-ph/0302149].
[2] C. S. Wood, S. C. Bennett, D. Cho, B. P. Masterson, J. L. Roberts, C. E. Tanner and C. E. Wieman, Science **275**, 1759 (1997).
[3] M. Gorchtein and C. J. Horowitz, Phys. Rev. Lett. **102**, 091806 (2009) [arXiv:0811.0614 [hep-ph]].
[4] A. Sibirtsev, P. G. Blunden, W. Melnitchouk and A. W. Thomas, Phys. Rev. D **82**, 013011 (2010) [arXiv:1002.0740 [hep-ph]].
[5] B. C. Rislow and C. E. Carlson, Phys. Rev. D **83**, 113007 (2011) [arXiv:1011.2397 [hep-ph]].
[6] M. Gorchtein, C. J. Horowitz and M. J. Ramsey-Musolf, Phys. Rev. C **84**, 015502 (2011) [arXiv:1102.3910 [nucl-th]].
[7] N. L. Hall, P. G. Blunden, W. Melnitchouk, A. W. Thomas and R. D. Young, Phys. Rev. D **88**, no. 1, 013011 (2013) [arXiv:1304.7877 [nucl-th]].
[8] N. L. Hall, P. G. Blunden, W. Melnitchouk, A. W. Thomas and R. D. Young, arXiv:1504.03973 [nucl-th].
[9] D. Wang *et al.* [Jefferson Lab Hall A Collaboration], Phys. Rev. Lett. **111**, no. 8, 082501 (2013) [arXiv:1304.7741 [nucl-ex]].
[10] T. Allison *et al.* [Qweak Collaboration], Nucl. Instrum. Meth. A **781**, 105 (2015) [arXiv:1409.7100 [physics.ins-det]].
[11] C. W. Leemann, D. R. Douglas and G. A. Krafft, Ann. Rev. Nucl. Part. Sci. **51**, 413 (2001).
[12] R. D. Young, R. D. Carlini, A. W. Thomas and J. Roche, Phys. Rev. Lett. **99**, 122003 (2007) [arXiv:0704.2618 [hep-ph]].
[13] R. D. Young, J. Roche, R. D. Carlini and A. W. Thomas, Phys. Rev. Lett. **97**, 102002 (2006) [nucl-ex/0604010].
[14] D. T. Spayde *et al.* [SAMPLE Collaboration], Phys. Lett. B **583**, 79 (2004) [nucl-ex/0312016].
[15] T. M. Ito *et al.* [SAMPLE Collaboration], Phys. Rev. Lett. **92**, 102003 (2004) [nucl-ex/0310001].
[16] K. A. Aniol *et al.* [HAPPEX Collaboration], Phys. Rev. Lett. **82**, 1096 (1999) [nucl-ex/9810012].
[17] K. A. Aniol *et al.* [HAPPEX Collaboration], Phys. Rev. Lett. **96**, 022003 (2006) [nucl-ex/0506010].
[18] K. A. Aniol *et al.* [HAPPEX Collaboration], Phys. Lett. B **635**, 275 (2006) [nucl-ex/0506011].

[19] A. Acha *et al.* [HAPPEX Collaboration], Phys. Rev. Lett. **98**, 032301 (2007) [nucl-ex/0609002].
[20] Z. Ahmed *et al.* [HAPPEX Collaboration], Phys. Rev. Lett. **108**, 102001 (2012) [arXiv:1107.0913 [nucl-ex]].
[21] D. S. Armstrong *et al.* [G0 Collaboration], Phys. Rev. Lett. **95**, 092001 (2005) [nucl-ex/0506021].
[22] D. Androic *et al.* [G0 Collaboration], Phys. Rev. Lett. **104**, 012001 (2010) [arXiv:0909.5107 [nucl-ex]].
[23] F. E. Maas *et al.* [A4 Collaboration], Phys. Rev. Lett. **93**, 022002 (2004) [nucl-ex/0401019].
[24] F. E. Maas *et al.*, Phys. Rev. Lett. **94**, 152001 (2005) [nucl-ex/0412030].
[25] S. Baunack *et al.*, Phys. Rev. Lett. **102**, 151803 (2009) [arXiv:0903.2733 [nucl-ex]].
[26] S. L. Zhu, S. J. Puglia, B. R. Holstein and M. J. Ramsey-Musolf, Phys. Rev. D **62**, 033008 (2000) [hep-ph/0002252].
[27] J. J. Kelly, Phys. Rev. C **70**, 068202 (2004).
[28] J. Beringer *et al.* [Particle Data Group Collaboration], Phys. Rev. D **86**, 010001 (2012).